Luminescent Solar Concentrators: Boosted Optical Efficiency by Polymer Dielectric Mirrors

G. Iasilli,[a] R. Francischello,[a] P. Lova,[b] S. Silvano,[b] A. Surace,[b] G. Pesce,[b] M. Alloisio,[b] M. Patrini,[c] M. Shimizu,[d] D. Comoretto,[b]* A. Pucci,[a]*

[a.] Dipartimento di Chimica e Chimica Industriale, Università di Pisa, via Moruzzi 13, 56124 Pisa, Italy. E-mail: davide.comoretto@unige.it

[b.] Dipartimento di Chimica e Chimica Industriale, Università di Genova, Via Dodecaneso 31, 16146 Genova, Italy. E-mail: andrea.pucci@unipi.it

[c.] Dipartimento di Fisica, Università di Pavia, via Bassi 6, 27100 Pavia, Italy

[d.] Faculty of Molecular Chemistry and Engineering, Kyoto Institute of Technology, 606-8585 Kyoto, Japan

SUPPORTING INFORMATION

Table of Contents

S1. Diffuser and LSC Characterization

The diffuser reflectance spectrum of the diffuser used in the reference device is reported in Figure S1a. In the spectral range of interest (500-800 nm, highlighted in grey) the reflectance of the diffuser is almost constant to a value of about 95%. Figure S1b shows instead the reflectance spectra of the LSC collected from the two sides of the slab. In both cases the reflectance approaches 6% in the near-infrared spectral region and undergoes a strong decrease at about 600 nm at the absorption onset of the fluorophore (Compare with Figure 1). The value at shorter wavelength is then lower from the side where the PMMA-fluorophore layer is casted.

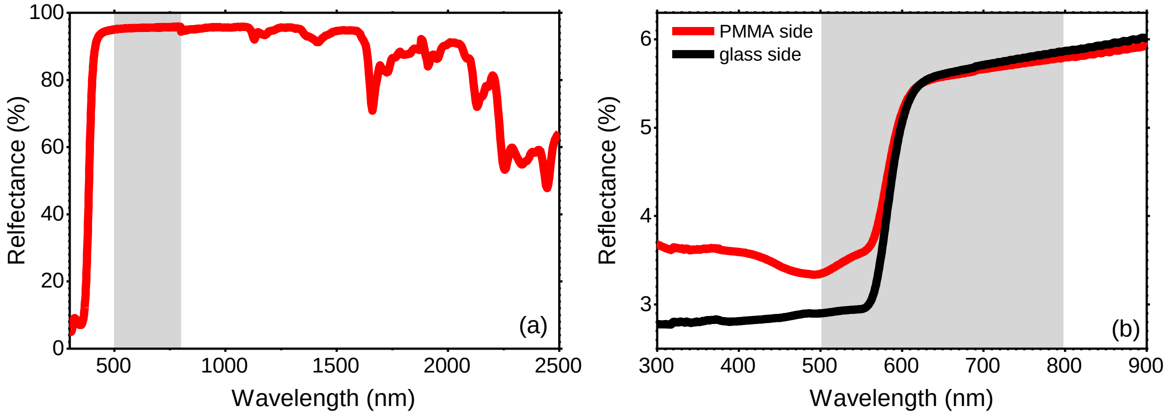

Figure S1. Reflectance spectra of (a) the diffuser and (b) the bare LSC collected from the PMMA side (red line) and from the glass side (black line).

S2: Hybrid Titania-PVA Nanocomposite Optical Functions

The optical functions of the new nanocomposite are compared with those of bare PVA in Figure S2. The real part (panel a) of the complex refractive index $\tilde{n}$=n+ik is described in the comment of Figure 2. In panel b instead, we notice that the extinction coefficient of the bare polymer (red line) is zero in the entire spectral range, indeed PVA is expected to be highly transparent in this spectral range. Once the HyTi is loaded into the polymer, the imaginary part of the refractive index start rising at 340 nm, testifying the effective load of the titania.[1]

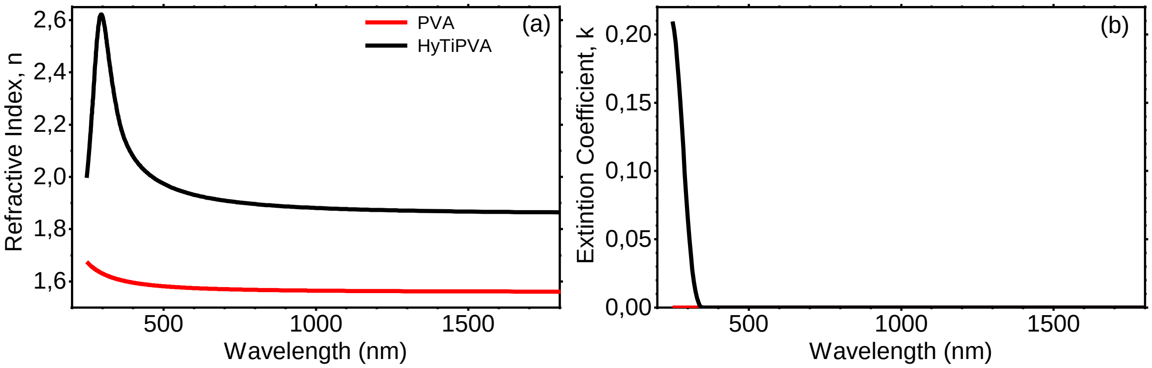

Figure S2 Real (a) and imaginary (b) part of the complex refractive index $\tilde{n}$=n+ik.

S3. Optical characterization of the DBRs

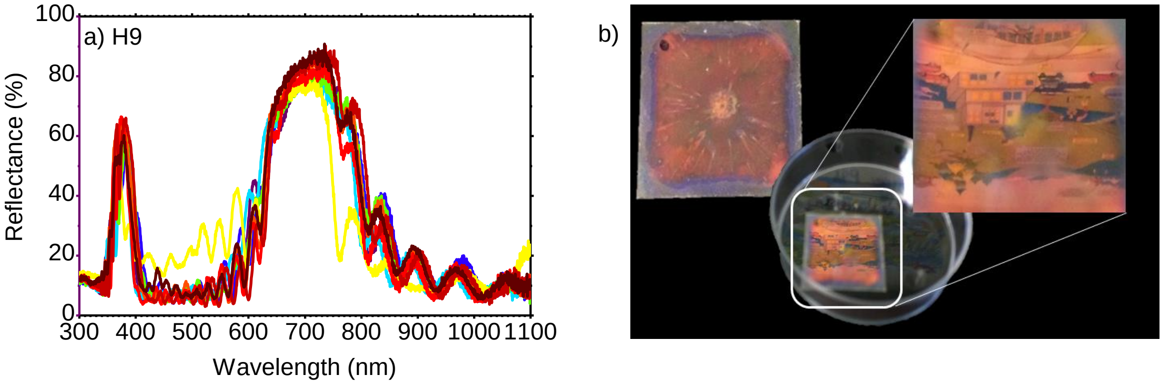

Figure S3. (a) Full spectral range reflectance spectra of sample H9. (b) Digital photographs of sample H1 sample at normal incidence top-left corner) and at about 30° (at the bottom in the center of the panel). The image in the top-right corner shows a magnification of an image reflected from the sample surface placed vertically at about 1m of distance.

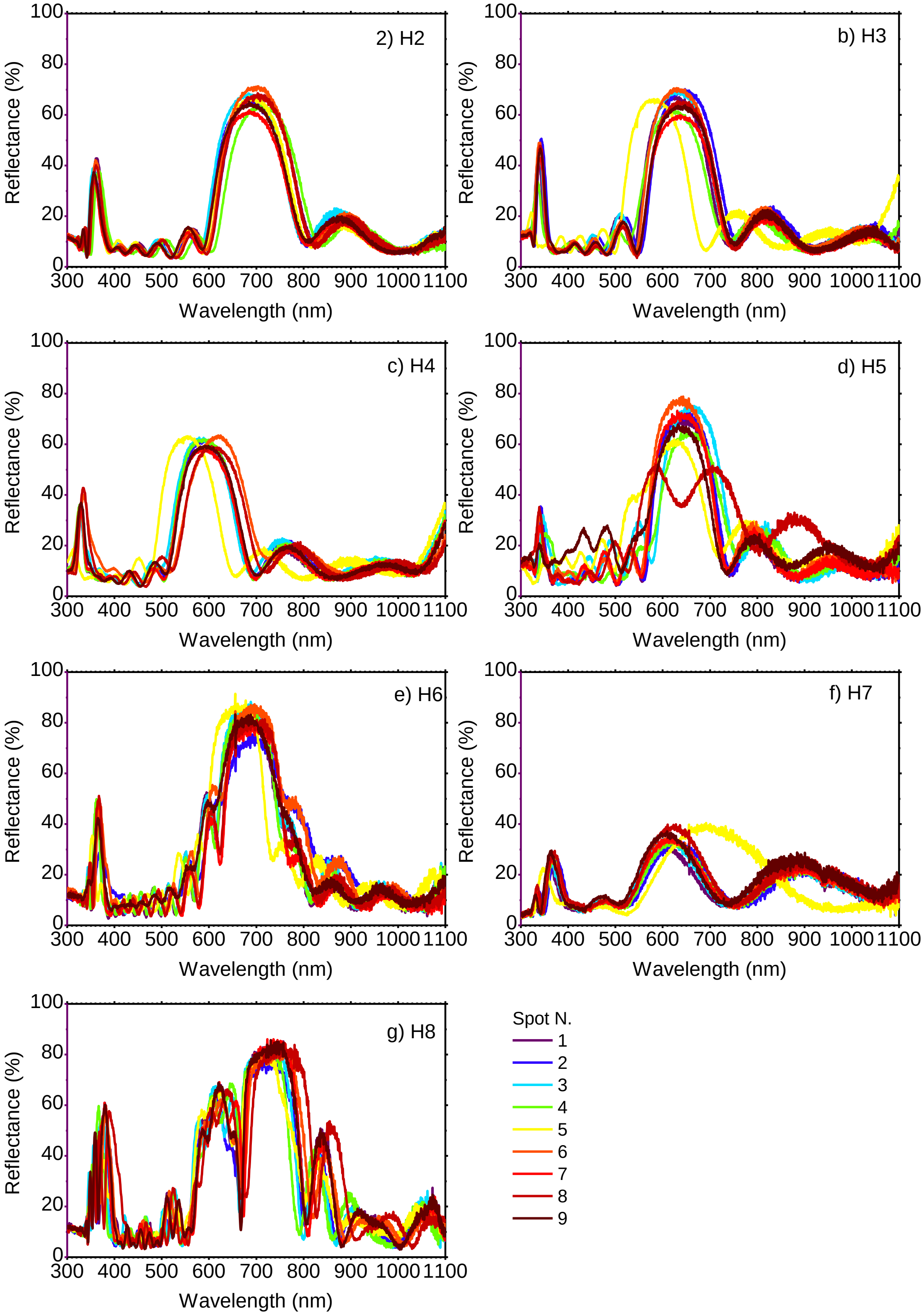

Figure S4. Reflectance spectra of H2-H8 samples investigated in this work. For sample details see Supporting Information Table S1, below.

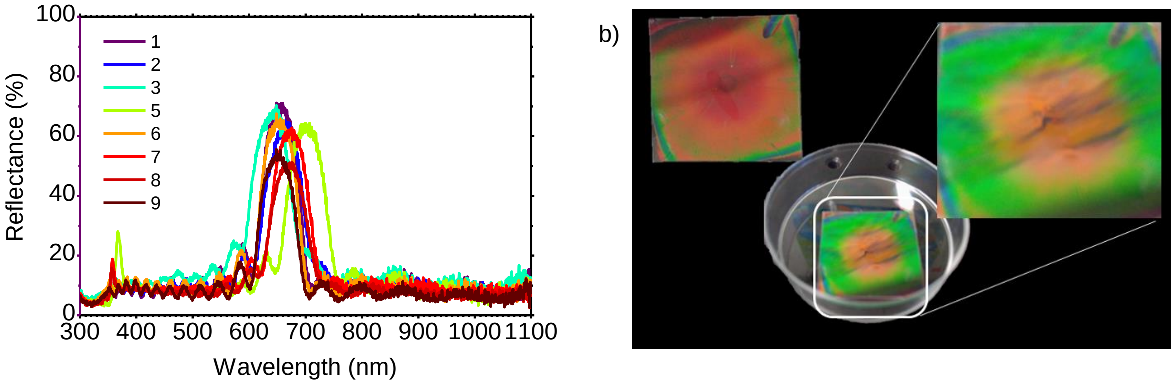

Figure S5. (a) Full spectral range reflectance spectra of sample P1. (b) Digital photographs of P1 sample at normal incidence top-left corner) and at about 30° (at the bottom in the center of the panel).

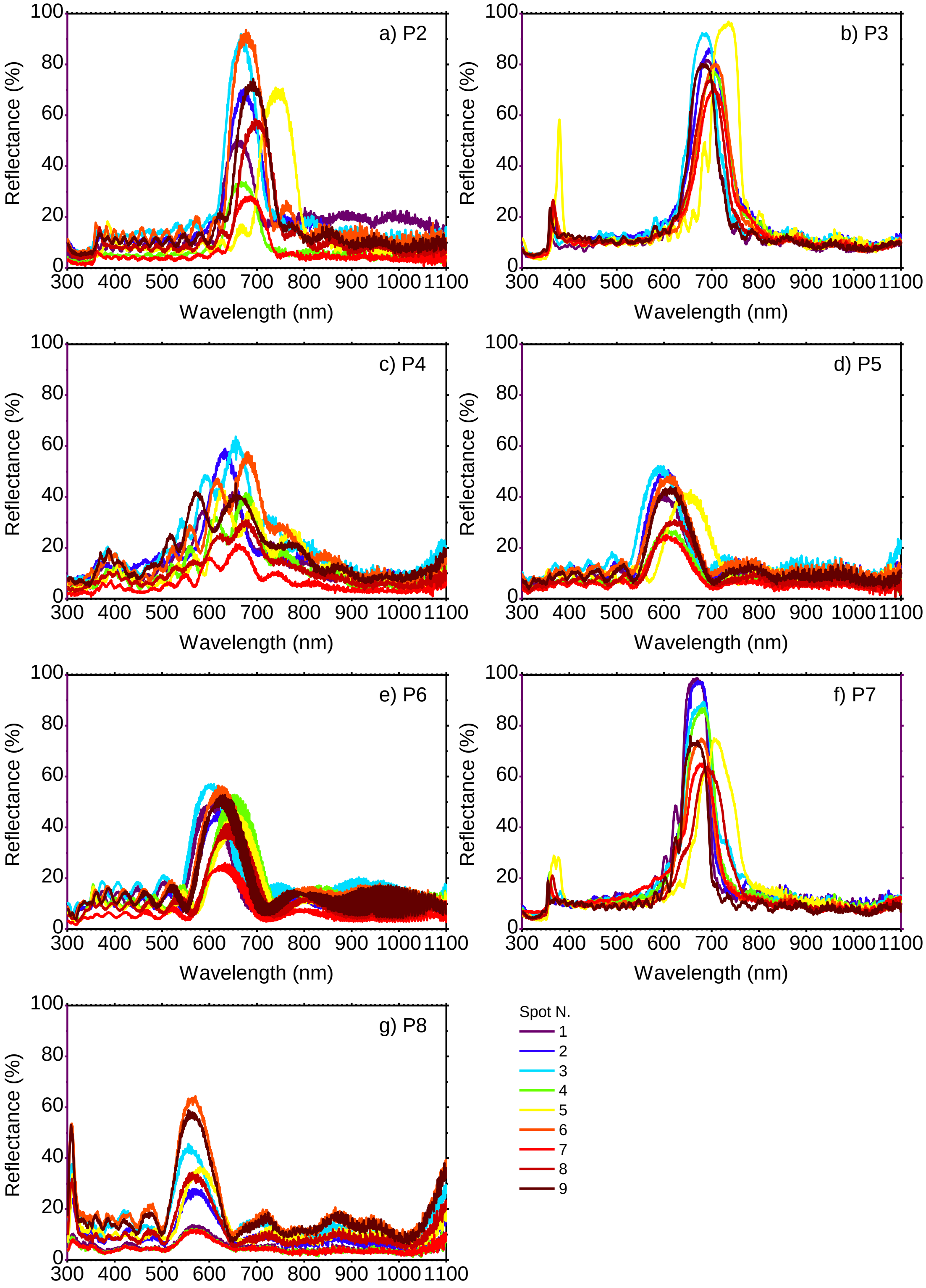

Figure S6. Reflectance spectra of P2-P8 samples investigated in this work. For sample details see Supporting Information Table S1, below.

Table S1: DBR fabrication parameters

DBR	N. of periods	Rotation speed (rps)
H1	15.5	80
H2	5.5	80
H3	5.5	100
H4	5.5	120
H5	6.5	80
H6	10.5	80
H7	3.5	80
H8	15.5	80
P2	12.5	80
P3	25.5	95
P4	12.5	100
P5	6.5	100
P1	12.5	100
P6	6.5	105
P7	24.5	100
P8	12.5	105

S4. Optical Efficiency Measurement Details

As mentioned in the manuscript, a home-built equipment setup was utilized to measure the efficiency of the solar collectors. Each DBR, single or mosaic (composed by four single DBRs) were placed beneath the LSCs of G = 8 or G = 16, respectively. Each sample was tested in triplicate. A sample holder with the photovoltaic (PV) module (IXYS SLMD121H08L mono solar cell 86 x 14 mm: Voc = 5.04 V, Isc = 50.0 mA, FF > 70%, ηPV = 22%, EQE Figure S6) is placed 2.5 cm above a scattering layer. The photovoltaic (PV) cell is masked with black tape to match LSC edge (50 x 3 mm) so that limiting the stray light to negligible levels. Silicon was used to grease the LSC edge. The other three edges of the LSC were covered with a reflective aluminum tape. A solar simulating lamp (ORIEL® LCS-100 solar simulator 94011A S/N: 322, AM1.5G std filter: 69 mW/cm-2 at 254 mm) was housed 27.5 cm above the sample. The PV module was connected to a digital potentiometer (AD5242) controlled via I2C by an Arduino Uno (https://www.arduino.cc) microcontroller using I2C master library. A digital multimeter (KEITHLEY 2010) was connected in series with the circuit, between the PV module and the potentiometer, to collect the current as a function of the external load. Conversely, the voltage was measured by connecting the multimeter in parallel to the digital potentiometer. Arduino Uno controlled the multimeter via SCPI language over RS-232 bus using a TTL to RS-232 converter chip (MAX232). Arduino Uno was connected to a computer via USB port and controlled by a Python script. The measurement cycle began with a signal from PC to Arduino which set the multimeter parameter to measure current. Then, Arduino began the measure loop: (1) set the potentiometer to a given value; (2) send a trigger signal to the multimeter; (3) read the measured data and (4) send the data back to PC. The loop is repeated 256 times for potentiometer values ranging 60 Ω to 1 MΩ. Arduino set the multimeter to measure voltage and for each potentiometer value the system recorded 8 data samples which were subsequently processed by the Python script. A schematic representation of the apparatuses used for photocurrent and photovoltage measurements is reported in Figures S7. The optical efficiency was reported as η_{opt} and obtained from the concentration factor (C), which is the ratio between the maximal current of the PV cell attached the LSC edges under illumination of the solar simulating lamp and the maximal current of the bare cell put perpendicular to the lamp.

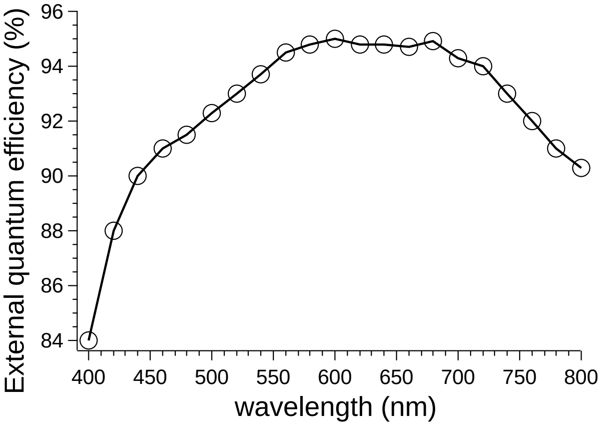

Figure S7. External quantum efficiency of the utilized Si-PV cell

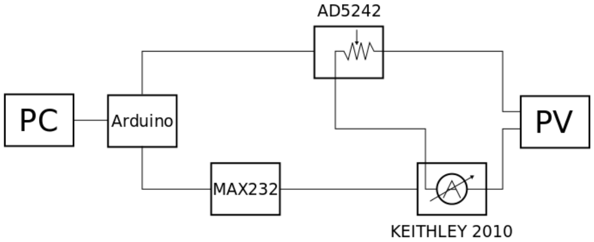

Figure S8. Scheme of the apparatus utilized for the photocurrent measurement

References:

(1) TiO_2 optical functions from Tauc-Lorentz oscillator in database of WVASE32® software by J. A. Woollam Co., I.